Annals of Clinical and Medical Case Reports

Case Report ISSN 2639-8109 Volume 7

Iron Deposit Central Large Nodule in Alagille Syndrome

Kim SK[1], Fujii T[1*], Kobayashi H[2], Okuda T[1], Fujii Y[1], Nakai A[1], Hayakumo T[1], Ohtani A[3], Koma Y[4], Kumabe T[5], Nakashima O[6], Yokoi A[7], Morisada N[8] and Kim SR[1]

[1]Department of Gastroenterology, Kobe Asahi Hospital, Kobe, Japan

[2]Department of Radiology, Kobe Asahi Hospital, Kobe, Japan

[3]Department of Pharmacy, Kobe Asahi Hospital, Kobe, Japan

[4]Division of Pathology, Department of Pathology, Kobe University Graduate School of Medicine, Kobe, Japan

[5]Kumabe Clinic, Kumamoto, Japan

[6]Department of Clinical Laboratory Medicine, Kurume University Hospital, Kurume, Japan

[7]Department of Pediatric Surgery, Hyogo Prefectural Kobe Children's Hospital, Kobe, Japan

[8]Department of Clinical Genetics, Hyogo Prefectural Kobe Children's Hospital, Kobe, Japan

[*]Corresponding author:

Takako Fujii,
Department of Gastroenterology, Kobe Asahi Hospital. 3-5-25 Bououji-cho, Nagata-ku, Kobe, 653-0801, Japan, Tel: +81-78-612-5151, Fax: +81-78-612-5152,
E-mail: kytacako@gmail.com

Received: 28 Jun 2021
Accepted: 13 July 2021
Published: 19 July 2021

Keywords:

Alagille syndrome; *JAG1* mutation; MRI T2-star W imaging; Paucity of bile ducts; Iron deposit central giant nodule

Citation:

Fujii T, Iron Deposit Central Large Nodule in Alagille Syndrome. Ann Clin Med Case Rep. 2021; V7(2): 1-7

1. Abstract

Alagille syndrome (ALGS) is a multisystem autosomal dominant disorder attributed to defects in the Notch signaling pathway. The mutation of Jagged 1 (*JAG1*) gene on chromosome 20 has been identified as the underlying cause of this syndrome. In addition, the mutation of Ryanodine receptor 2 (*RYR2*) gene on chromosome 1 has clarified. Here described is a 7 × 5 cm nodular lesion in segment 4 in a 28-year-old man with ALGS. Through imaging studies and histopathological analysis, the nodule was diagnosed, for the first time, as iron deposit giant nodule. Additionally, a review of previous reports has been made to shed more light on this syndrome.

2. Introduction

Alagille syndrome (ALGS), acknowledged as arteriohepatic dysplasia, is a multisystem autosomal dominant disorder attributed to defects in the Notch signaling pathway [1, 2]. The mutations of Jagged 1 (*JAG1*) gene on chromosome 20 that encodes a ligand for the Notch receptor, have been known as the basic cause of this syndrome. Hepatic involvement is one of its main clinical features of chronic cholestasis attributed to paucity of interlobular bile ducts. Progressive liver disease, leading to liver cirrhosis occurs in about 15% of cases and may require liver transplantation (LT) [1-7]. These patients are at risk of hepatocellular carcinoma (HCC), therefore early detection of HCC is critical in the follow-up of this disease [7].

This study describes the case of a 28-year-old man with a 7 × 5 cm nodular lesion in segment 4 compatible with iron deposit central large nodule detected by radiological and histopathological analysis. We also review previous reports that describe solitary focal hepatic nodules adjacent to the right portal vein as large regenerative hyperplasia.

3. Case Reports

3.1. Chief Complaint

A 28-year-old man with ALGS was admitted to our hospital for further evaluation of a liver tumor.

3.2. Physical Examination

On admission, the patient displayed slight jaundice without hepatomegaly, weighed 40.4 kg, stood 154.5 cm tall, and had a BMI of 16.9.

His characteristic facies featured a prominent forehead, moderate hypertelorism with deep-set eyes, a small chin, and a saddle or straight nose. Computed tomography (CT) revealed butterfly-like forms in the lumbar vertebra (L4) (Fig. 1a). Although the patient's mother demonstrated similar facial features, she had normal liver function and no liver tumor; however, she has been undergoing renal dialysis of unknown etiology for seven years.

3.3. History of Past Illness

During his neonatal period, the patient had meconium peritonitis and an atrial septum defect, but no heart surgery or blood transfusion.

3.4. Laboratory Examinations

Laboratory data on admission were shown in Table 1.

Electrocardiogram (ECG) and Holter ECG were normal without QT prolongation. Ultrasonic cardiogram (UCG) showed no abnormality (Table 1).

Table 1: Laboratory data on admission

WBC	6200 $\times 10^3$/μl	(39-98)	transferrin	232 mg/dl	(190-320)
Hb	14.6 g/dl	(13-18)	ferritin	416 ng/ml	(12-275)
Platelets	29.0 $\times 10^4$/μl	(12-30)	ANA	40 IU/ml	(≦40)
PT	88.30%	(70-130)	AMA	1.5 IU/ml	(≦20)
TP	8.2 g/dl	(6.5-8.3)	IgG	1376mg/dl	(870-1700)
ALB	4.2 g/dl	(3.8-5.3)	IgA	432mg/dl	(110-410)
T-bil	2.73 mg/dl	(0.2-1.3)	IgM	143 mg/dl	(33-190)
AST	169 IU/l	(≦38)	HBsAg	(－)	
ALT	104 IU/l	(≦19)	HCVAb	(－)	
ALP	1098 IU/l	(38-126)	AFP	2.4 ng/ml	(≦10.0)
γ-GTP	4049 IU/l	(≦40)	CEA	2.7 ng/ml	(≦5.0)
Fe	128 μg/dl	(54-200)	PIVKA-II	51 mAU/ml	(≦40)
			CA19-9	7.8 U/ml	(≦37)

WBC, white blood cell; Hb, hemoglobin; PT, prothrombin time; TP, total protein; ALB, albumin; T-bil, total bilirubin; AST, aspartate aminotransferase; ALT, alanine aminotransferase; ALP, alkaline phosphatase; γ-GTP, gamma-glutamyl transpeptidase; Fe, ferrum; ANA, antinuclear antibody; AMA, antimitochondrial antibody; IgG, immunoglobulin G; IgA, immunoglobulin A; IgM, immunoglobulin M; HBsAg, hepatitis B surface antigen; HCVAb, hepatitis C virus antibody; AFP, alpha-fetoprotein; CER, carcinoembryonic antigen; PIVKA-II, Protein induced by Vitamin K absence-II; CA19-9, carbohydrate antigen 19-9.

3.5. Imaging Examinations

Ultrasound (US) revealed a 7 × 5 cm isoechoic nodule in segment 4 (Fig. 1b).

Contrast-enhanced US (CEUS) revealed no enhancement in the arterial phase and no defect in the Kupffer phase. Unenhanced CT revealed a slightly high-attenuation nodule (Fig. 1c). Contrast-enhanced computed tomography (CECT) revealed the right portal vein adjacent to the nodule and the portal vein (P4) (Fig. 1d) and middle hepatic veins through the nodule (Fig. 1e), but no enhancement in the arterial phase and no defect in the late phase. Gadolinium-ethoxybenzyl diethylenetriamine pentaacetic acid (Gd-EOB-DTPA)-enhanced magnetic resonance imaging (MRI) revealed no enhancement in the arterial phase, and no defect in the hepatobiliary phase.

From above radiological findings, hypervascular tumors such as focal nodular hyperplasia (FNH), adenoma, cholangiolocellular carcinoma (CoCC), HCC, hemangioma, bile duct adenoma (BDA), lymphoproliferative disorders including pseudolymphoma were ruled out.

MRI revealed signal loss on T1 weighted imaging (T1WI) in-phase (Fig. 1f) com-pared with T1WI opposed-phase (Fig. 1g), hypointensity on fat-suppressed T2 weighted imaging (T2WI-FS) (Fig. 1h), and marked hypointensity on diffusion-weighted imaging (DWI) and the apparent diffusion coefficient (ADC) map respectively. The nodule was markedly hypointense on T2-star weighted imaging (T2*WI) (Fig. 1i) and on superparamagnetic iron oxide (SPIO) enhanced MRI.

Based on these MRI findings, an iron deposit tumor was suspected.

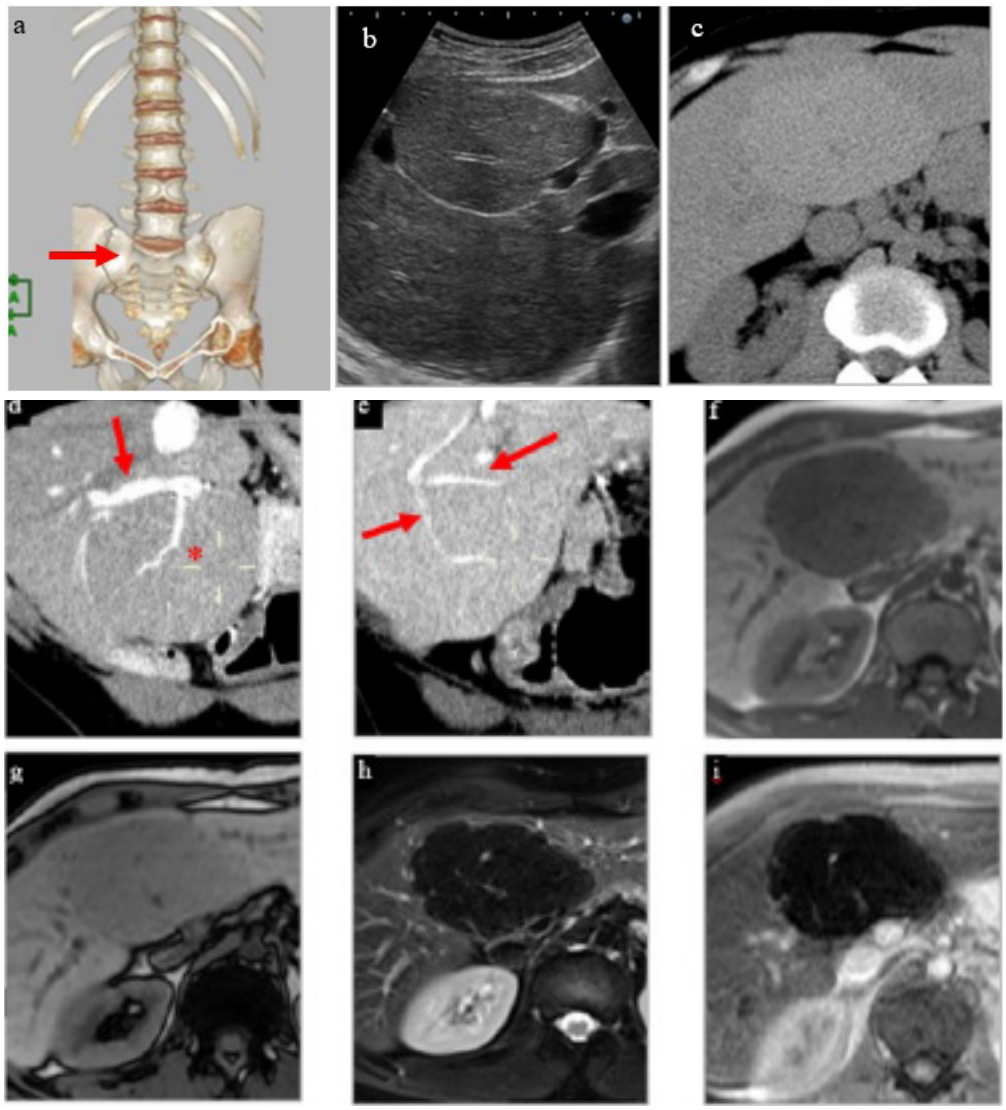

Figure 1: Imaging findings.
a: CT revealed butterfly-like forms in the lumbar vertebra in L4; b: US reveals a 7 x 5 cm isoechoic nodule in S4; c: CT reveals a 7 x 5 cm slightly high-attenuation nodule in S4; d: CECT reveals the right portal vein (arrow) adjacent to the nodule and the portal vein (P4) (asterisk) through the nodule. (coronal image); e: CECT reveals the middle hepatic veins (arrows) through the nodule. (coronal image); f, g: MRI reveals signal loss on T1WI in-phase (f) compared with on T1WI opposed-phase (g); h: MRI reveals hypointensity on fat-suppressed T2WI; i: MRI reveals marked hypointensity on T2*WI.

3.6. Histopathological Examinations

US guided biopsy of the nodule revealed normal portal tracts including bile duct, artery and portal vein. Parenchymal hepatocytes showed no remarkable hyperplastic change compared with the background of the liver or the non-nodular lesion (Fig. 2a, b, c).

Immunohistopathological studies revealed positive findings of organic anion-transporting polypeptide (OATP), and normal or negative findings of glutamine synthetase (GS), C-reactive protein (CRP), liver fatty acid binding protein (L-FABP), β-catenin, heat shock protein (HSP) and glypican-3 (GPC3). In terms of the nodule FNH, adenoma, nodular regenerative hyperplasia and HCC were ruled out.

US guided biopsy of the background revealed no remodeling of lobular architecture with stage 1 fibrosis, and the portal tract contained no bile ducts. Parenchymal hepatocytes showed hyperplastic change with increased cell density and irregular cell cords (Fig. 2d, e, f). The above findings were compatible with ALGS.

Berlin blue staining revealed abundant hemosiderin deposits in both the hepatocyte cytoplasm and Kupffer cells in the nodule (Fig. 2g), but not in the background of the liver (Fig. 2h).

3.7. Final Diagnosis

Based on the above findings and histopathological analysis, the lesion was diagnosed as iron deposit nodule.

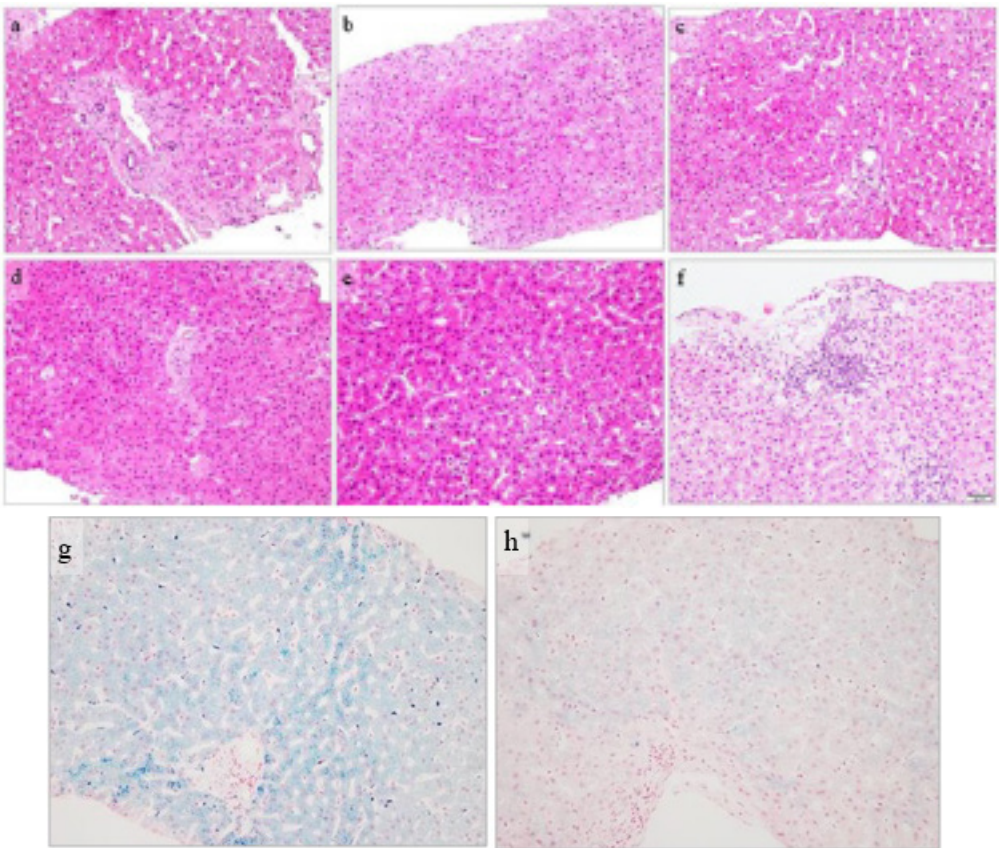

Figure 2: Histopathological findings

a, b, c: Normal portal tracts including bile duct, artery and portal vein are observed in the nodule. Parenchymal hepatocytes of nodular area show no remarkable hyperplastic change compared with the background of the liver. (HE staining, ×100); d, e, f: No remodeling of lobular architecture with stage 1 fibrosis, but each portal tract contains no bile duct is observed in the non-nodular lesion. Parenchymal hepatocytes show hyperplastic change with increased cell density and irregular cell cords. (HE staining, ×100); g: Hemosiderin deposits in the Kupffer cells and hepatocyte cytoplasm are observed in the nodule. (Berlin blue staining, ×100); h: No hemosiderin deposits in the Kupffer cells and hepatocyte cytoplasm are observed in the non-nodular lesion. (Berlin blue staining, ×100).

3.8. Genetic examinations

To identify the molecular diagnosis, genetic analysis of the patient was carried out. All procedures were reviewed and approved by the Institutional Review Boards of Kobe Asahi Hospital and Kobe University School of Medicine (No.86).

After written informed consent from the patient and his family, DNA was extracted from peripheral blood mononuclear cells by using the Quick Gene Mini 80 system (Wako Pure Chemical Industries, Ltd., Tokyo, Japan). Next generation sequencing was carried out with the use of the TruSight One Sequencing (TS1) Panel (Illumina, San Diego, CA, USA), which can analyze 4,813 genes.

Genetic analysis revealed heterozygous NM_000214.2: c.703 T > C at *JAG1* (Fig. 3a), and heterozygous NM_001035.2: c.3358 T > C at Ryanodine receptor (*RYR2*) (Fig. 3b) in the patient. DNA from the patient's mother showed the same missense variant in *JAG1* (Fig. 3a) but no variant in *RYR2* (Fig. 3b). No sequence alterations were observed in the coding regions of HFE, HAMP, TFR2, SLC40A1, BMP2 and FTH1 genes in the context of hemochromatosis (Data not shown).

4. Discussion

The diagnosis of ALGS is essentially clinical, specified by chronic cholestasis and congenital heart disease. Classic criteria, based on the 5 main systems have been reported: cholestasis due to bile duct paucity, congenital heart disease (most commonly peripheral pulmonary artery stenosis), the face (mild but recognizable dysmorphic features), the eye (most commonly posterior embryotoxon), and the skeleton (most commonly butterfly vertebrae). It is thought that the diagnosis is reasonable if bile duct paucity is accompanied by 3 of the 5 main criteria [7-9]. In our case, bile duct paucity accompanied by the 5 main clinical criteria were established, leading to the diagnosis of ALGS [1].

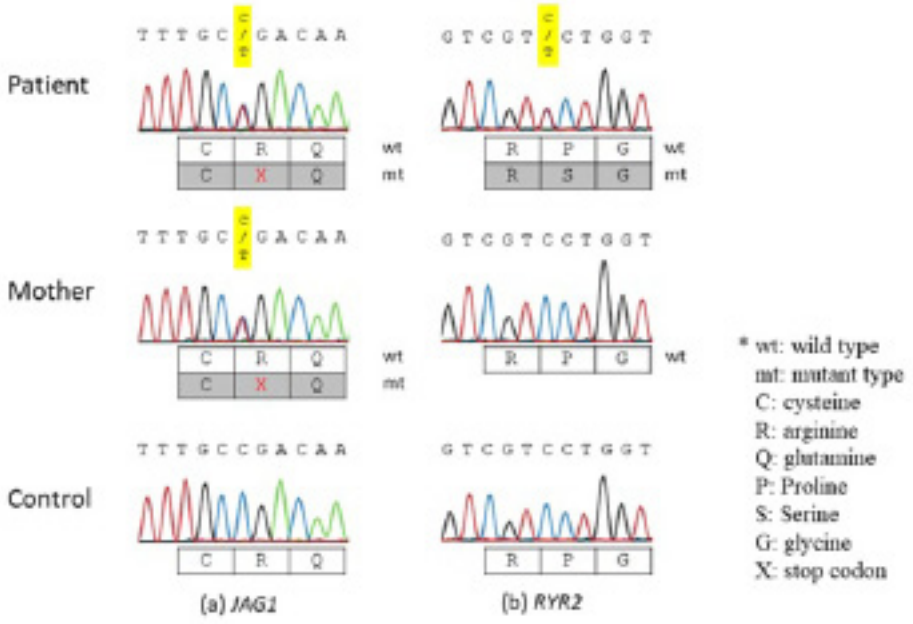

Figure 3: Genetic analysis of the patient and his mother
(a): The mutations of Jagged 1 (*JAG1*) gene; (b): The mutation of Ryanodine receptor 2 (*RYR2*) gene.

In our case, heterogeneous NM_000214.2: c.703T>C at *JAG1* related to Notch signaling was seen in the patient and his mother, and the autosomal dominant hereditary disorder was established. Moreover, the heterogeneous NM_001035.2: c.3358T>C at *RYR2* gene related to catecholaminergic polymorphic ventricular tachycardia (CPVT) without was seen in the patient, whereas his mother demonstrated no variants in *RYR2*. CPVT, an inherited arrhythmic disorder characterized by bidirectional or polymorphic tachycardia caused by exercise or emotional stress [10], is reported to be as high as 1:10000, but its real prevalence is unclear [11].

To the best of our knowledge, the present is the first report of the *RYR2* variant seen in ALGS. It is not clear whether *JAG1* and *RYR2* variants are linked to ALGS. Further data on gene analysis of ALGS cases are necessary.

Paucity of interlobular bile ducts in the liver seems to advance through infancy and is thought a key feature, reported in 80-90% of a large series. It does not, however, always develop in worsening of hepatic function and advancement of liver cirrhosis [1]. In our case, liver cirrhosis was not seen in either the nodular or the non-nodular lesion, although paucity of interlobular bile ducts in the portal area was seen in the non-nodular lesion.

Based on MRI findings, iron deposit nodule was first considered then confirmed by histopathological findings, making this, to the best of our knowledge, the first report on iron deposit nodule in ALGS.

MRI findings of iron overload, particularly in the liver, are well reported [12]. Hepatic iron overload is abnormal accumulation of iron in hepatocytes, Kupffer cells, or both [13, 14]. Hepatic iron overload is commonly related to hereditary hemochromatosis, transfusion-related iron overload, and chronic hepatopathy. MRI is the selected modality for the detection of hepatic iron [15].

Iron leads to local distortion in the magnetic field, which results in T1, T2, and T2*-W shortening. This results in signal loss on T2 weighted spin-echo/fast spin-echo imaging and gradient echo T2*WI, and is applied for the measurement of iron concentration. Since iron-induced T2*-W shortening is superior to iron-induced T2 shortening, T2*WI provides greater sensitivity in detecting iron, and is more commonly applied for this purpose.

From previous reports it is unclear whether the nodules with iso-to-hyperintensity on T1WI and hypointensity on T2WI are iron deposit nodules, because findings on T1WI in phase and T1WI opposed-phase images have not been described therein [1, 11, 15-18].

Primary iron overload (i.e., hereditary hemochromatosis) is an autosomal recessive disorder in which a defective protein leads to increased intestinal absorption of iron from the small intestine at 5-10 times the normal rate. Secondary iron overload syndromes include iron loading anemias (i.e., thalassemia, sideroblastic anemia, sickle cell disease, chronic hemolytic anemia, aplastic anemia, pyruvate kinase deficiency), chronic liver diseases (i.e., hepatitis C infection, non-alcoholic fatty liver disease, alcoholic fatty liver disease), and iatrogenic (i.e., red blood cell transfusion, long-term hemodialysis) and various causes [15]. In our case, regarding the iron deposit nodule, hereditary hemochromatosis was denied through gene testing. The patient had no history of blood transfusion and demonstrated no other secondary overload syndrome, irrespective of slight elevated level of serum ferritin (416 ng/ml).

Further study is needed to clarify the reason for the presence of iron deposits exclusively in the nodule observed in our case.

In ALGS hepatic nodules display less fibrosis and relatively well preserved interlobular bile ducts than the rest of the liver that shows either extensive fibrosis or liver cirrhosis [19]. In our case, the nodule was seen adjacent to the right portal vein, was located in the central zone of the liver, as in previous reports [1, 16, 18-21], and revealed relatively well preserved interlobular bile ducts without fibrosis, whereas the rest of the liver or non-nodular lesion revealed paucity of bile ducts with stage 1 hepatic fibrosis.

Similar findings are reported in explanted livers after Kasai portoenterostomy [19]. At the molecular level, *JAG1* mosaicism and differential haploinsufficiency do not clarify the presence of bile ducts in centrally located regenerative nodules in ALGS [19].

All masses (nodules) in previously described similar pediatric cases have been lesions larger than 5 cm [16]. In our case, the size of the nodule (7 × 5 cm) is compatible with that in previous reports [1, 16, 18-21].

The histological differential diagnosis of mass liver lesions in ALGS includes malignancies, such as HCC and hepatoblastoma, as well as benign proliferative tumors such as hepatic adenoma and FNH [18]. To date, 19 cases of ALGS -associated liver tumors have been reported in the literature including 15 cases of HCC [4, 7, 9, 18, 22-29].

In our case, based on histopathological and radiological findings, HCC, liver adenoma and FNH were ruled out. Also, no primitive cell population of hepatoblastoma was seen.

Sublobular nodules of hepatocytes free of iron or exhibiting much less iron than the adjacent parenchyma, referred to as iron-free-foci (IFF), are frequently demonstrated in the livers of patients with genetic hemochromatosis complicated by HCC [30].

5. Conclusion

That study clearly demonstrates that IFF nodules are proliferative lesions strongly suggestive of preneoplastic foci.

In our case, hemochromatosis was ruled out on the basis of gene analysis. Nonetheless, the iron deposit nodule diagnosed through histopathological analysis differed from HCC. The non-iron deposit portion, or IFF, in the non-nodular lesion showing hyperplastic change with increased cell density and irregular cell cords may be a risk factor of HCC, as in hemochromatosis.

The eventuality of the occurrence of HCC needs to be monitored continually in cases of iron deposit nodules.

6. Conflicts of Interest

None of the authors has any conflict of interest.

7. Funding Disclosure

This research received no external funding.

8. Acknowledgments

The authors thank Ms. Mika Matsui for excellent technical assistance.

References

1. Ennaifer R, Farhat LB, Cheikh M, Romdhane H, Marzouk I, Belhadj N, et al. Focal liver hyperplasia in a patient with Alagille syndrome: Diagnostic difficulties. A case report. Int J Surg Case Rep. 2016; 25: 55-61.
2. Turnpenny PD, Ellard S. Alagille syndrome: pathogenesis, diagnosis and management. Eur J Hum Genet. 2012; 20: 251-7.
3. Alagille D, Estrada A, Hadchouel M, Gautier M, Odievre M, Dommergues JP, et al. Syndromic paucity of interlobular bile ducts (Alagille syndrome or arteriohepatic dysplasia): review of 80 cases. J Pediatr. 1987; 110: 195-200.
4. Kaufman SS, Wood RP, Shaw BW, Markin RS, Gridelli B, Vanderhoof JA, et al. Hepatocellular carcinoma in a child with Alagille syndrome. Am J Dis Child. 1987; 141: 698-700.
5. Tsai S, Gurakar A, Anders R, Lam-Himlin D, Boitnott J, Pawlik TM, et al. Management of large hepatocellular carcinoma in adult patients with Alagille syndrome: a case report and review of literature. Dig Dis Sci. 2010; 55: 3052-8.
6. Kim B, Park SH, Yang HR, Seo JK, Kim WS, Chi JG, et al. Hepatocellular carcinoma occurring in alagille syndrome. Pathol Res Pract. 2005; 201: 55-60.
7. Torizuka T, Tamaki N, Fujita T, Yonekura Y, Uemoto S, Tanaka K, et al. Focal liver hyperplasia in Alagille syndrome: assessment with hepatoreceptor and hepatobiliary imaging. J Nucl Med. 1996; 37: 1365-7.
8. Emerick KM, Rand EB, Goldmuntz E, Krantz ID, Spinner NB, Piccoli DA, et al. Features of Alagille syndrome in 92 patients: frequency and relation to prognosis. Hepatology. 1999; 29: 822-829.
9. Adams PC. Hepatocellular carcinoma associated with arteriohepatic dysplasia. Dig. Dis. Sci. 1986; 31: 438-42.
10. Saito A, Ohno S, Nuruki N, Nomura Y, Horie M, Yoshinaga M, et al. Three cases of catecholaminergic polymorphic ventricular tachycardia with prolonged QT intervals including two cases of compound mutations. J Arrhythm. 2018; 34: 291-3.
11. Sumitomo N. Current topics in catecholaminergic polymorphic ventricular tachycardia. J Arrhythm. 2016; 32: 344-51.
12. Andrade QM, Blasbalg R, Ortega CD, Rodstein MAM, Baroni RH, Rocha MS, et al. MR imaging findings of iron overload. Radiographics. 2009; 29: 1575-89.
13. Brittenham GM, Cohen AR, McLaren CE, Martin MB, Griffith PM, Nienhuis AW, et al. Hepatic iron stores and plasma ferritin concentration. Am J Hematol. 1993; 42: 81-5.
14. St Pierre TG, Clark PR, Chua-Anusorn W. Single spin-echo proton transverse relaxometry of iron-loaded liver. NMR Biomed. 2004; 17: 446-58.

15. Idilman IS, Akata D, Ozmen MN, Karcaaltincaba M. Different forms of iron accumulation in the liver on MRI. Diagn Interv Radiol. 2016; 22: 22-8.

16. Rapp JB, Bellah RD, Maya C, Pawel BR, Anupindi SA. Giant hepatic regenerative nodules in Alagille syndrome. Pediatr Radiol. 2017; 47: 197-204.

17. Sandhu K, Flintoff K, Chatfield MD, Dixon JL, Ramm LE, Ramm GA, et al. Phenotypic analysis of hemochromatosis subtypes reveals variations in severity of iron overload and clinical disease. Blood. 2018; 132: 101-10.

18. Tajima T, Honda H, Yanaga K, Kuroiwa T, Yoshimitsu K, Irie H, et al. Hepatic nodular hyperplasia in a boy with Alagille syndrome: CT and MR appearances. Pediatr Radiol. 2001; 31: 584-8.

19. Rougemont AL, McLin VA. Central Liver Nodules in Alagille Syndrome and Biliary Atresia After Kasai Portoenteros-tomy. J Pediatr Gastroenterol Nutr. 2016; 63: 41-2.

20. Alhammad A, Kamath BM, Chami R, Ng VL, Chavhan GB. Solitary Hepatic Nodule Adjacent to the Right Portal Vein: A Common Finding of Alagille Syndrome? J Pediatr Gastroenterol Nutr. 2016; 62: 226-32.

21. Roberts P, Trout AT, Dillman JR. Nodular macroregenerative tissue as a pattern of regeneration in cholangiopathic disorders. Pediatr Radiol. 2018; 48: 932-40.

22. Bekassy AN, Garwicz S, Wiebe T, Hagerstrand I, Jensen OA. Hepatocellular carcinoma associated with arteriohepatic dysplasia in a 4-year-old girl. Med Pediatr Oncol. 1992; 20: 78-83.

23. Tuset E, Ribera JM, Domenech E, Vaquero M, Oller B, Armengol M, et al. Pseudotumorous hyperplasia of the caudate lobe of the liver in a patient with Alagille syndrome. Med Clin (Barc). 1995; 104: 420-2.

24. Bail BL, Bioulac-Sage P, Arnoux R, Perissat J, Saric J, Balabaud C, et al. Late recurrence of a hepatocellular carcinoma in a patient with incomplete Alagille syndrome. Gastroenterology. 1990; 99: 1514-6.

25. Nishikawa A, Mori H, Takahashi M, Ojima A, Shimokawa K, Furuta T. ALAGILLE'S SYNDROME A Case with a Hamartomatous Nodule of the Liver. Acta Pathol Jpn. 1987; 37: 1919-26.

26. Ong E, Williams SM, Anderson JC, Kaplan PA. MR imaging of a hepatoma associated with Alagille syndrome. J Comput Assist Tomogr. 1986; 10: 1047-9.

27. duCret RP, Cefalu JB, Alford BA, Drake G, Boudreau RJ. Hepatocarcinoma in association with the Alagille syndrome. Clin Nucl Med. 1988; 13: 920-1.

28. Chiaretti A, Zampino G, Botto L, Polidori G. Alagille syndrome and hepatocarcinoma: a case report. Acta Paediatr. 1992; 81: 937.

29. Torbenson MS, Ng IOL, Park YN, Roncalli M, Sakamoto M. Digestive System Tumours. WHO Classification of Tumours. 5th Edition. Hepatocellular carcinoma; International Agency for Research on Cancer: Geneva, Switzerland, 2019; 229-39.

30. Deugnier YM, Charalambous P, Quilleuc DLe, Turlin B, Searle J, Brissot P, et al. Preneoplastic significance of hepatic iron-free foci in genetic hemochromatosis: a study of 185 patients. Hepatology. 1993; 18: 1363-9.